

Supporting Information

Lattice-strained metal-organic frameworks synthesized by microwave assisted promote oxygen evolution reaction

Caiyao Yan^{a,*}, Hongfeng Wu^{a,b}

^aInstitute for Materials Discovery, University College London, London WC1E 7JE, United Kingdom

^b School of Materials and Chemical Engineering, Anhui Jianzhu University, Hefei, 230601 (P.R.China)

*Corresponding author: Caiyao Yan

E-mail addresses: qflinustc@163.com

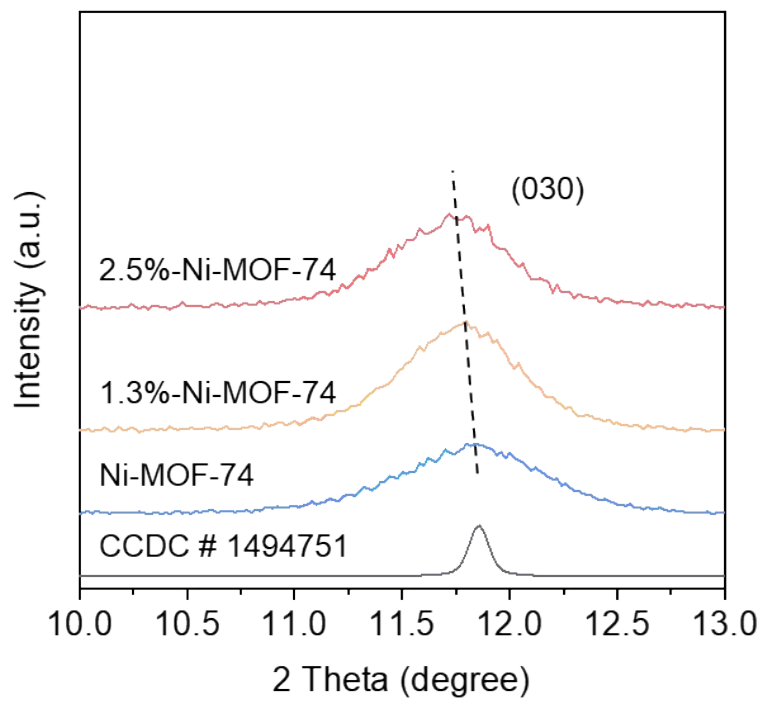


Fig. S1. XRD pattern for Ni-MOF-74, 1.3%-Ni-MOF-74 and 2.5%-Ni-MOF-74 of (030) plane.

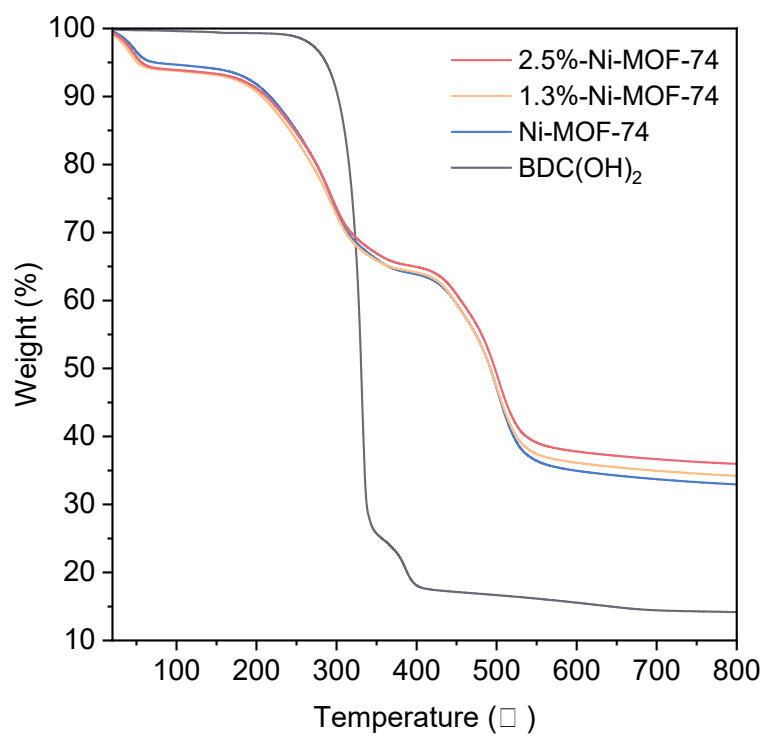


Fig. S2. TG diagram of the as synthesized MOFs and BDC(OH)₂.

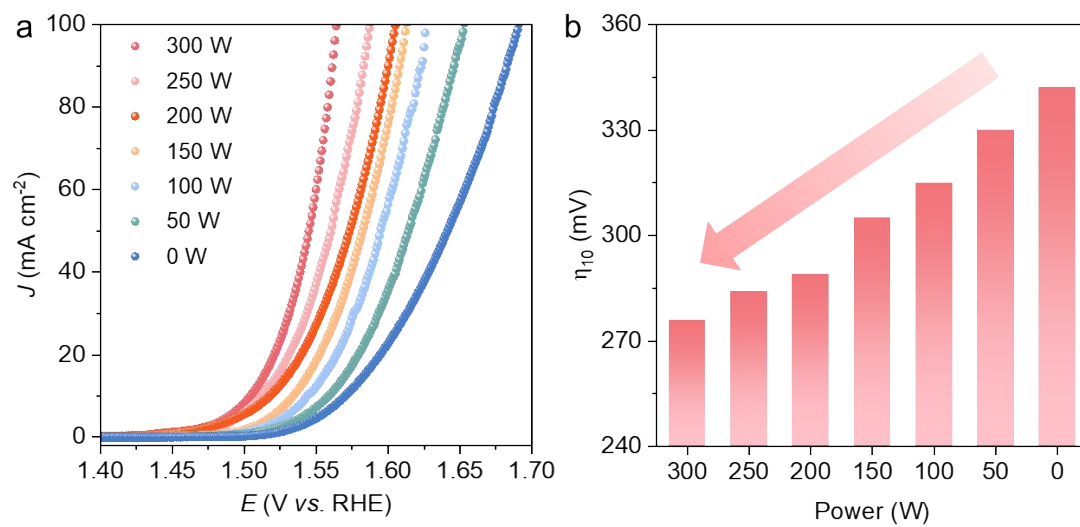


Fig. S3. (a) Linear sweep voltammetry curves of as synthesized Ni-MOF-74 with different powers and (b) the corresponding overpotential of 10 mA cm⁻².

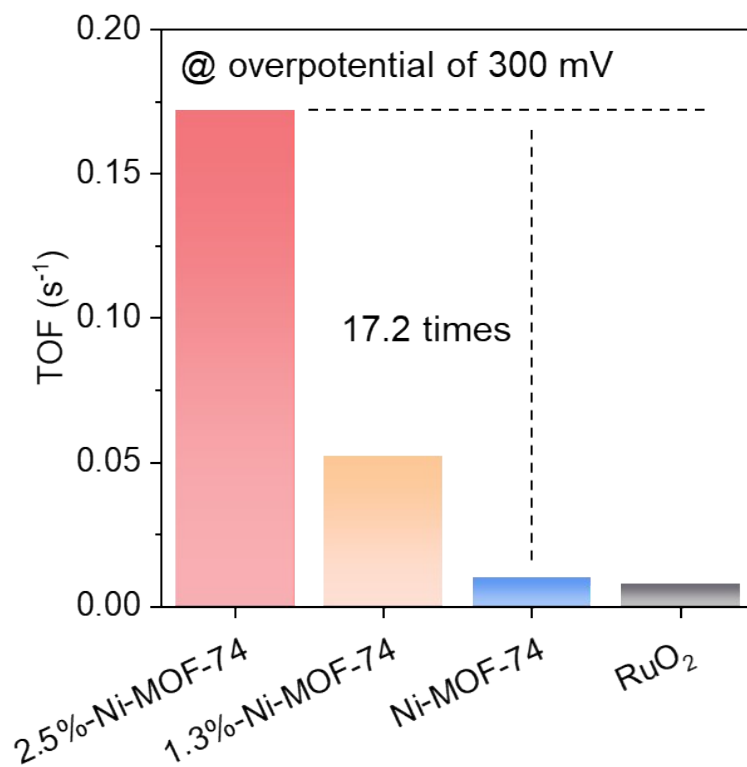


Fig. S4. TOF of OER for the Ni-MOF-74, 1.3%-Ni-MOF-74 and 2.5%-Ni-MOF-74 and RuO₂ at overpotential of 300 mV.

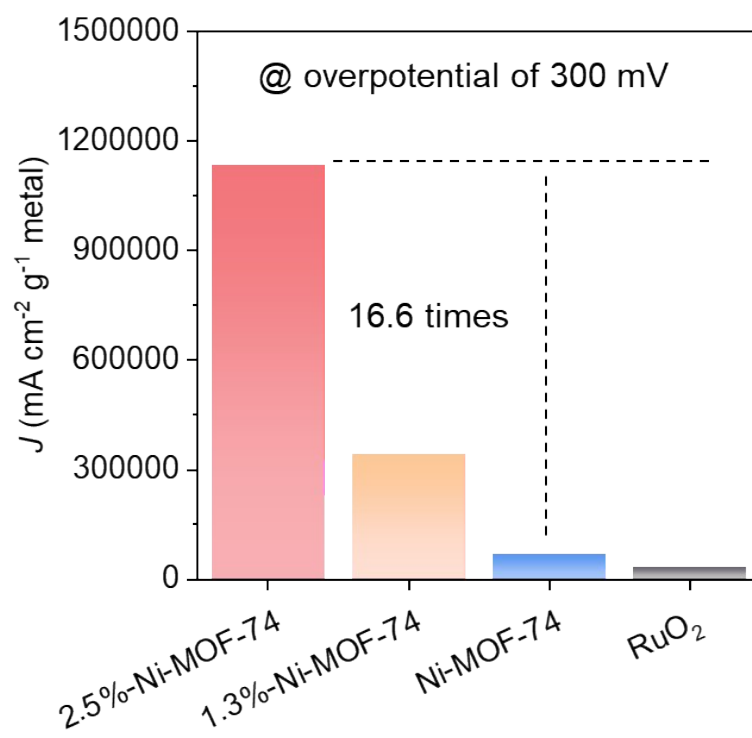


Fig. S5. Mass activity of OER for the Ni-MOF-74, 1.3%-Ni-MOF-74 and 2.5%-Ni-MOF-74 and RuO₂ at overpotential of 300 mV.

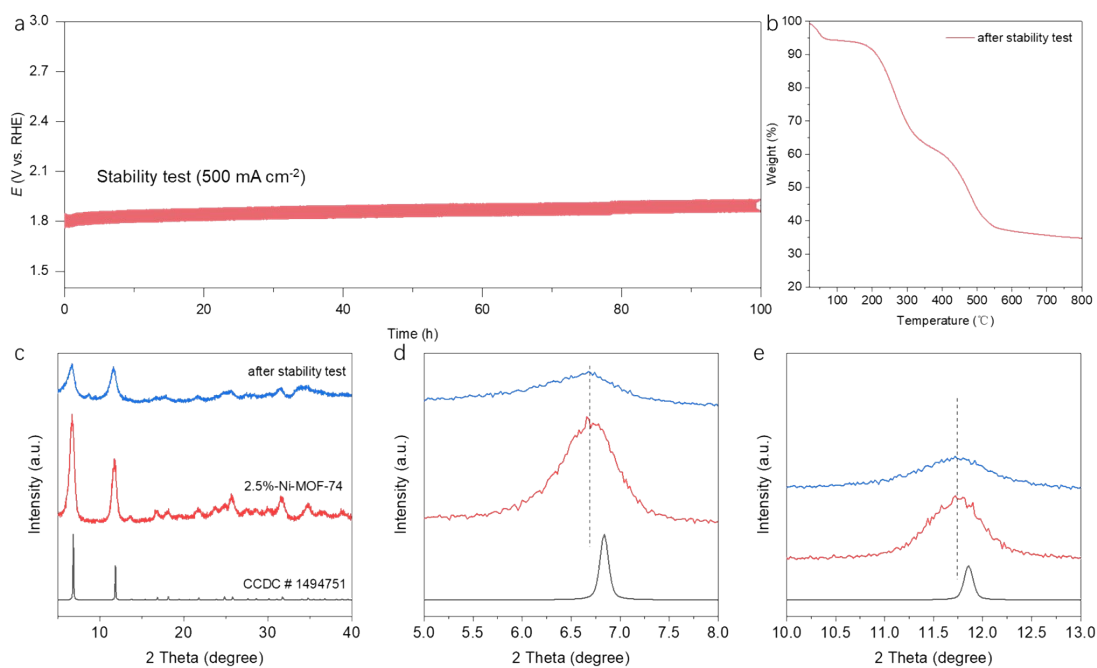


Fig. S6. (a) Stability test again of 2.5%-Ni-MOF-74 measured in 1 M KOH using a H-type cell at 500 mA cm^{-2} . (b) TG diagram of 2.5%-Ni-MOF-74 after stability test (100 h @ 500 mA cm^{-2}). (c)-(e) XRD pattern of 2.5%-Ni-MOF-74 after the stability test.

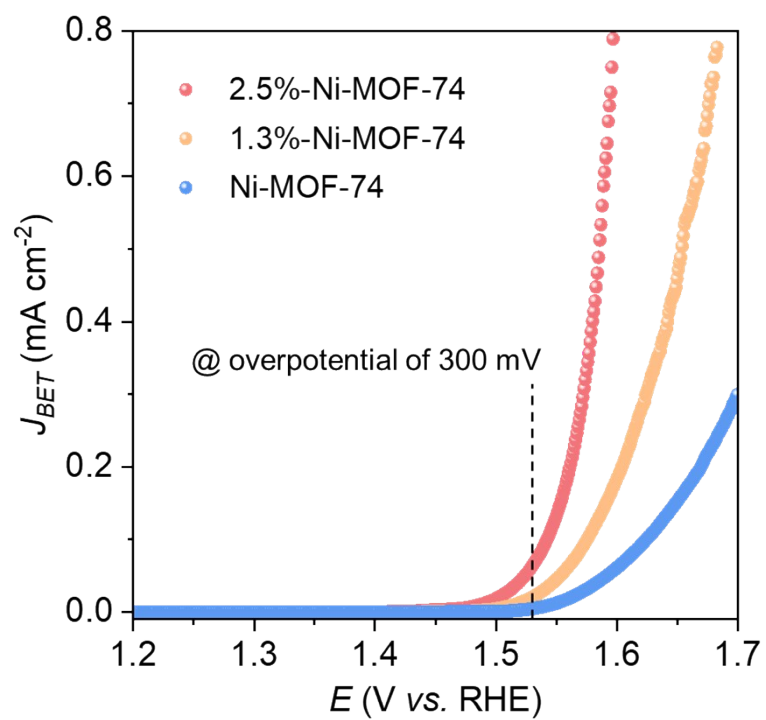


Fig. S7. Specific activity of OER normalized by surface area.

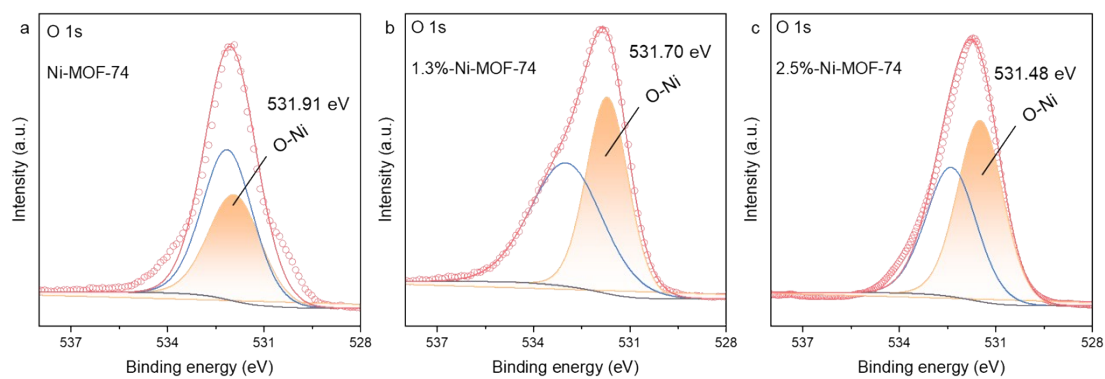


Fig. S8. Fitted O 1s XPS spectra of the (a) Ni-MOF-74, (b) 1.3%-Ni-MOF-74 and (c) 2.5%-Ni-MOF-74.

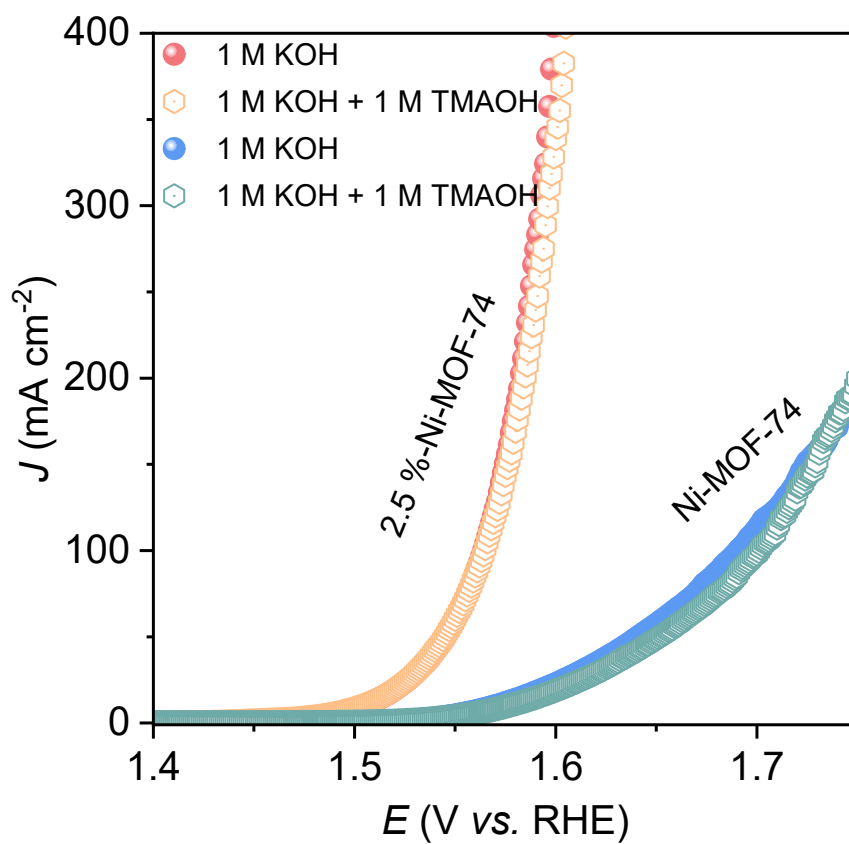


Fig. S9. Linear sweep voltammetry curves of 2.5%-Ni-MOF-74 and Ni-MOF-74 nanoplates in 1 M KOH and 1 M KOH + 1 M TMAOH solutions.

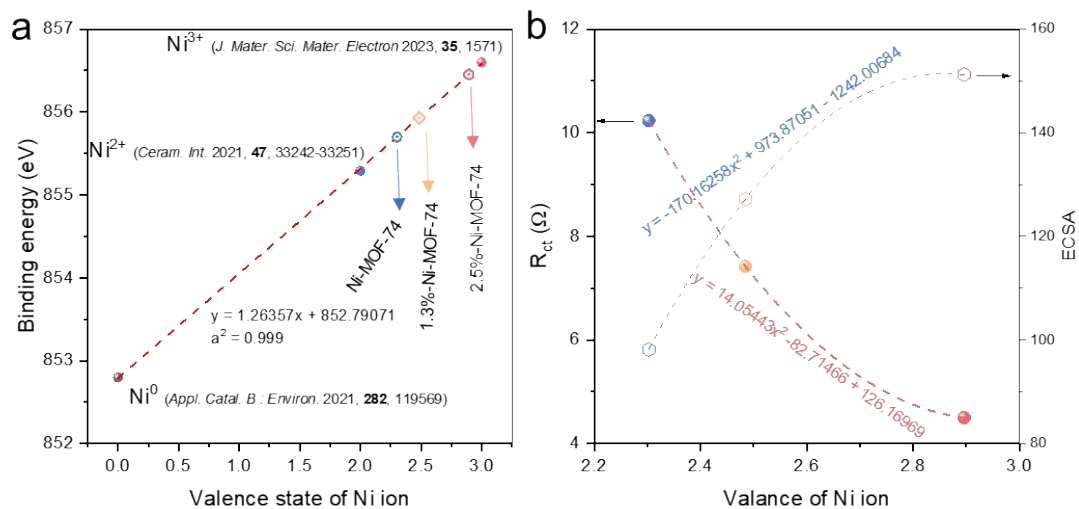


Fig. S10. (a) The valence state of Ni fitted based on the reported XPS results. (b) Mathematical models of Ni valence states between R_{ct} and ECSA respectively.

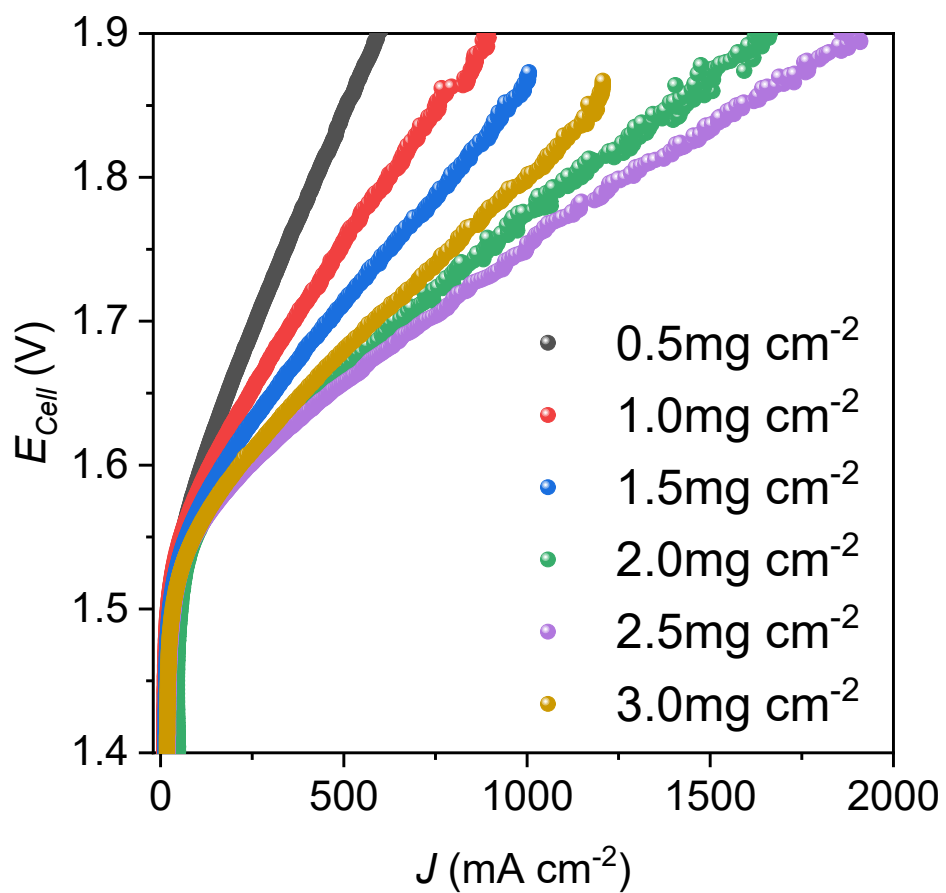


Fig. S11. LSV curves of anodes with different loading capacities.

Table S1. The Ni contents of catalysts, measured by ICP-OES.

| Catalyst | Ni content (wt. %) |
|-----------------|---------------------------|
| Ni-MOF-74 | 24.33 |
| 1.3%-Ni-MOF-74 | 23.46 |
| 2.5%-Ni-MOF-74 | 23.67 |

Table S2. The TOF and MA of catalysts.

| Catalyst | TOF (s ⁻¹) @ 300 mV | MA (A g ⁻¹ metal) @ 300 mV |
|------------------|---------------------------------|---------------------------------------|
| Ni-MOF-74 | 0.172 | 1133.580 |
| 1.3%-Ni-MOF-74 | 0.052 | 344.032 |
| 2.5%-Ni-MOF-74 | 0.01 | 68.779 |
| RuO ₂ | 0.008 | 32.969 |

Table S3. The C_{dl} of catalysts.

| Catalyst | 2.5%-Ni-MOF-74 | 1.3%-Ni-MOF-74 | Ni-MOF-74 |
|---------------------------------|-----------------------|-----------------------|------------------|
| C_{dl} (mF cm ⁻²) | 7.54 | 6.36 | 4.91 |
| ECSA= C_{dl}/C_s | 151.2 | 127.2 | 98.2 |

Table S4. The EIS of catalysts.

| Catalyst | R_s ($\Omega \text{ cm}^{-2}$) | R_{ct} ($\Omega \text{ cm}^{-2}$) |
|----------------|------------------------------------|---------------------------------------|
| 2.5%-Ni-MOF-74 | 1.71 | 4.50 |
| 1.3%-Ni-MOF-74 | 1.68 | 7.42 |
| Ni-MOF-74 | 1.55 | 10.23 |

Table S5. Comparison of OER performance between 2.5%-Ni-MOF-74 and reported catalysts in literatures.

| Catalysts | η_{10} (mV) | Tafel slope (mV dec ⁻¹) | Substrate | Stability (h) @ J (mA cm ⁻²) | Ref. |
|---|---------------------|--|--------------|---|---|
| 2.5%-Ni-MOF-74 | 276 | 54.6 | Carbon paper | 290 @ 500 | This work |
| Fe(OH) ₃ @Co-MOF-74 | 292 | 44 | GCE | 20 @ 50 | <i>ChemSusChem.</i> 2019, 12 , 4623-4628 |
| FeCo-MNS-1.0 | 298 | 21.6 | NF | 14 @ ~120 | <i>Angew. Chem. Int. Ed.</i> 2019, 58 , 13565-13572 |
| NiO-MOF-74 | 320 | 105 | GCE | 10 @ 10 | <i>J. Mater. Chem. A</i> 2018, 6 , 18720-18727 |
| Co _{0.6} Fe _{0.4} -MOF-74 | 280 | 56 | RDE | 12 @ ~12 | <i>ACS Energy Lett.</i> 2018, 3 , 2520-2526 |
| Fe-MOFs | 283 | 41.6 | NF | 24 @ 100 | <i>ChemCatChem.</i> 2021, 13 , 4976-4984 |
| (U+S)-CoFe-MOF | 277 | 31 | GCE | / | <i>ACS Sustain. Chem.</i> <i>Eng.</i> 2019, 7 , 16629- 16639 |
| Ni-BDC@NiS | 330 | 62 | Ni | 12 @ 20 | <i>ACS Appl. Mater. Inter.</i> 2019, 11 , 41595-41601 |